



Nano-synthesis, spectroscopic characterisation and antibacterial activity of some metal complexes derived from Theophylline



Ahmad H. Ismail¹, Hassanain K. Al-Bairmani¹, Zainab Sabri Abbas¹, Ahmed Mahdi Rheima^{2*}

¹ Mustansiriyah University, College of Science, Department of Chemistry, Iraq.

² Wasit University, College of Science, Department of Chemistry, Kut, Iraq.*

Abstract

The novel was assembled by the ultrasonic sonication method of three new ligand-metal nano complexes with Ni(II), Cu(II), and Co(II) of theophylline derivative. This method was used to produce smaller, small distributed nanoparticles and without any aggregations. Molar conductance, FT-IR, ¹HNMR, UV-Vis., solubility, flame atomic absorption, and (C.H.N) elemental analysis were used to describe and to suggest the structure of the new ligand and nanocomplexes. Engagement of all spectroscopic data indicates that the new ligand (L) acts as a bidentate ligand with its metal ions. The molar conductance reveals that the nanocomplexes were non-electrolytes. The size and morphology of nano complexes measured by TEM were in range (12-18) nm.

The biological activities of the synthesised metal nano complexes were assayed against four types of bacterial strains, *Staphylococcus aureus*, *Bacillus subtilis* (gram-positive bacteria) and *Klebsiella pneumonia*, *Escherichia Coli* (gram-negative bacteria). The results show remarkable leverage compared to the parent ligand in the present nano complexes.

Keywords: Nanocomplexes, new ligand, theophylline derivative, Ultrasonic Sonication, bacterial strains, TEM.

1. Introduction

Purines include Theophylline (Scheme 1), an organic compound that is a significant type of anti-inflammatory drug [1]. Theophylline has biological significance because it is structurally linked to the elements in nuclear acids [2]. Research into theophylline complexes shows that the purine base is mostly bonded to the metal ions in the N7 atom [3-8], Theophylline is, in a

few situations, a bident ligand, where the metal bond to the N7 is complemented by interaction with the O6 atom, which forms N7 / O6 chelation [9,10]. The research on nanotechnology enables the creation of new nanomaterials in a nanoscale below 100 nm [11-18]. The particular physical and chemical characteristics of nanomaterials are common in all areas [19-23]. The nano complexes have appropriate physical, chemical, and biological applications as studies have shown [24,25].

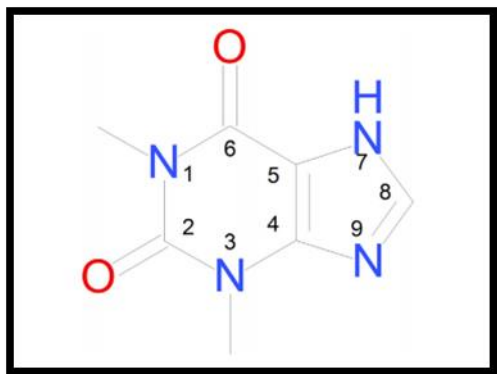
*Corresponding author e-mail: arahema@uowasit.edu.iq.

Receive Date: 13 June 2020, Revise Date: 04 July 2020, Accept Date: 13 July 2020

DOI: 10.21608/EJCHEM.2020.32582.2690

©2020 National Information and Documentation Center (NIDOC)

Transition metal complexes (TMCs) are cationic, neutral, or anionic types of metal in which ligands coordinate a transition metal [26]. They can be designed with the necessary adjustments of either the core metal or the ligand sphere for a specific function [27]. Transition metals show different oxidation states and can react with several negatively charged molecules. Research has shown essential advances in the use of transition metal complexes as drugs to treat many human diseases, where transition metal complexes are the most widely utilised chemotherapeutic agents and make a significant contribution to medicinal therapeutics [28]. The aim of this study has been reported to the synthesis and characterisation of Ni(II), Cu(II) and Co(II) nanocomplexes with theophylline derivative as a ligand for antibacterial applications.



Scheme 1. Structural Theophylline

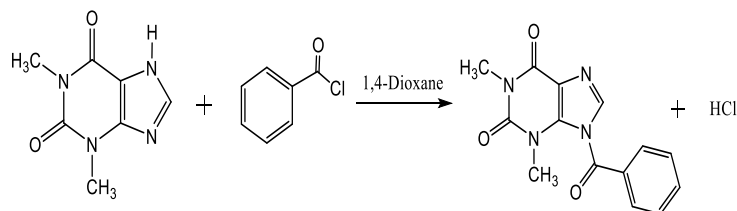
2. Experimental

2.1 Materials and methods

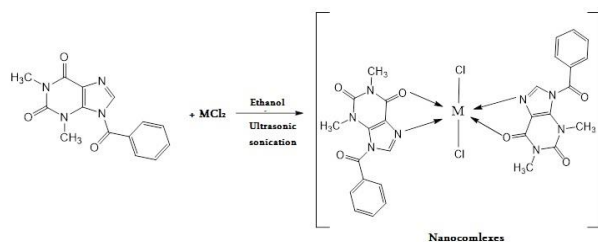
Sigma-Aldrich has purchased all chemicals and solvents applied. Deionised water was used through the preliminary steps.

2.2 Synthesis of new Ligand (7-benzoyl-1,3-dimethyl-3,7-dihydro-1H-purine-2,6-dione) and nanocomplexes

Three nanocomplexes of the metal ions of Ni(II), Cu(II), and Co(II) with Ligand were synthesised using the ultrasonic sonication method [5]. The new ligand was synthesised according to the process as shown in (Scheme 2). Theophylline (0.01 mole) was dissolved in 40 ml of dioxane. Then, benzoyl chloride (0.01 mole) was mixed with the obtained solution. The mixture was stirred and refluxed for 5 hr at 105 °C. The solution was cooled for 30 minutes in an ice bath. Brawn participated was isolated and washed several times with hot water. Finally, it was dried in the oven at 60 °C for 2 h. The nanocomplexes of Ni²⁺, Cu²⁺, and Co²⁺ with new ligand were prepared as shown in (Scheme 3) by dissolve (0.002 mole) of a ligand in 25 mL of ethanol, then metals (II) chloride (0.001 mol in 25 ml ethanol) were added to obtain a solution. The reaction mixture was kept under ultrasonic with reflux-heated for three hours at 50 °C. Appropriate crystals of good quality emerged at room temperature incubation after night. Filtration was used to isolate all complexes, wash with ethanol and dry on air [5].



Scheme 2. Syntheses of the 7-benzoyl-1,3-dimethyl-3,7-dihydro-1H-purine-2,6-dione.



Scheme 3 Nanoscale complexes synthesized [M= Ni(II), Cu(II) and Co(II)].

2.3 Characterisation

Some devices were used to characterised the metal nano complexes and ligand. TEM was used to measure the size and morphology of metal complexes. Molar Conductivity, FT-IR, ¹HNMR, solubility, flame atomic absorption, and (C.H.N) Elemental analysis was determined to investigate and suggest the structure of ligand and its metal nano complexes.

2.4 Antibacterial test

The antibacterial activity of the ligand and nanocomplexes have been tested against the Gram-negative bacteria such as *Klebsiella pneumonia*, *Escherichia Coli*, and Gram-positive bacteria such as *Staphylococcus aureus*, *Bacillus subtilis*. Accordingly, 10⁻³ M solutions were prepared by dissolving the appropriate weights of the selected metal nano complexes in dimethyl sulfoxide (DMSO) in addition to pure ligand solution of the same concentration. The prepared solutions were then used to examine their antibacterial activity using the agar diffusion method. The estimated number of bacteria cells in the agar dish by the McFarland norm was 1.5x10⁸ colonial units per milliliter. A cavity was made in each plate at a diameter of (5 mm) to fill with the solution of the metal nano complexes. The plates were incubated for 24 hours at 37 °C. The diameters of the resulting inhibition zones were measured and tabulated [29-31].

3. Results and discussion

3.1 FT-IR spectra

The new Ligand (L) serves as a bident, as its structure indicates. The nanocomplexes behaviour of the ligand with [Co(II), Ni(II), and Cu(II)] metal ions was well indicated as predicted by FT-IR. In comparison to the free ligand sites involved in chelation, the FTIR spectra of new ligand and complexes are expected to change in coordination in the position of some guide bands in the free Ligand (L) spectrum (Fig. 1-4). In Ligand (Fig.1) at 1681.98 and 1600.97 cm⁻¹, both (ν C=O) and (ν C=N) were detected, this shows that oxygen (O6) and nitrogen (N7) atoms were coordinated with metal ions.

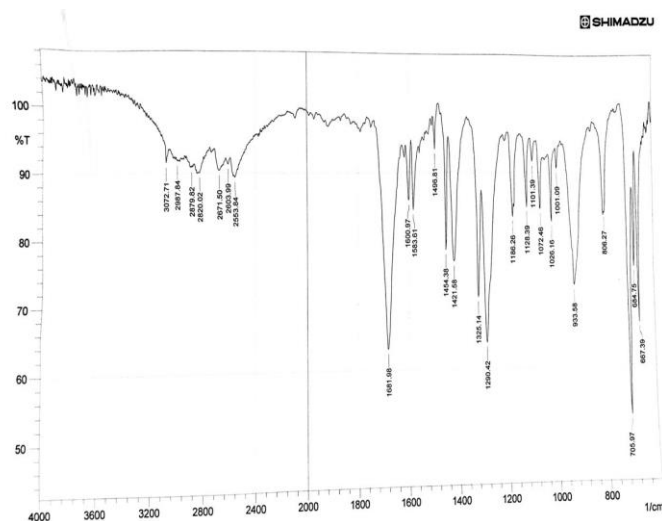


Fig. 1 FTIR spectrum of new Ligand (L).

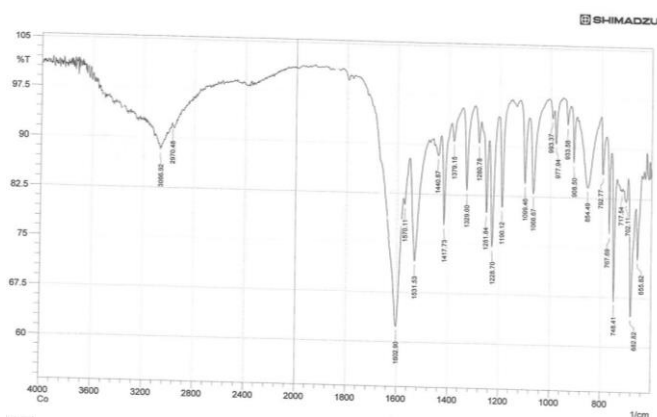


Fig. 2 FT-IR spectrum of the $[\text{Co}(\text{L})_2(\text{Cl})_2]$ nanocomplex.

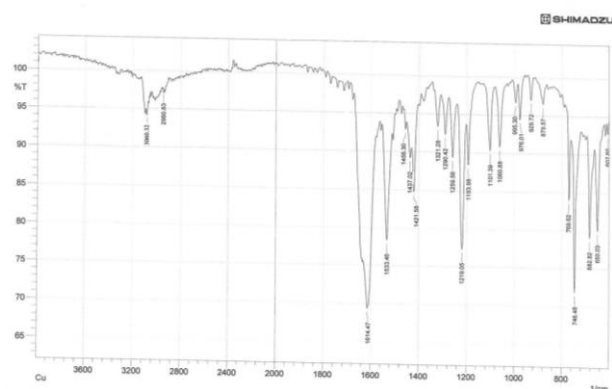


Fig. 3 FT-IR spectrum of the $[\text{Ni}(\text{L})_2(\text{Cl})_2]$ nanocomplex.

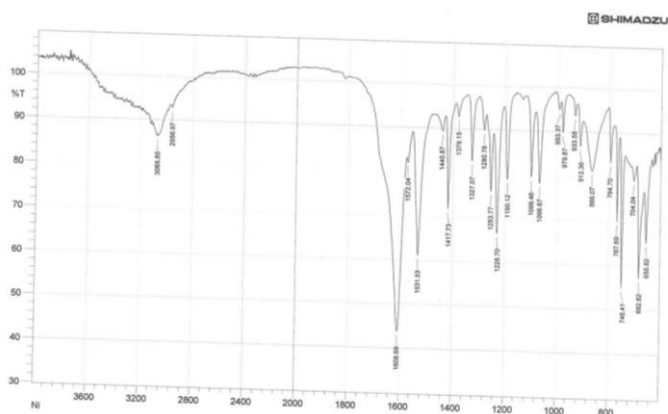


Fig. 4 FT-IR spectrum of the $[\text{Cu}(\text{L})_2(\text{Cl})_2]$ nanocomplex.

3.1.1 UV-visible spectra of the ligand and nanocomplexes

The electronic ligand spectrum and nanocomplexes are displayed in (Figs. 5-8) DMSO solution at room temperatures between 200-800 nm in length. The U.V-Vis spectrum of the free Ligand (Fig. 5) shows a 274 nm (36497 cm^{-1}) absorbent band insolvent (DMSO) to which this band is attributable to ($\pi - \pi^*$).

The U.V-Vis spectrum of $[\text{Co}(\text{L})_2(\text{Cl})_2]$ complex (Fig. 6), exhibits two peaks at 579 nm (17271 cm^{-1}) and 530 nm (18867 cm^{-1}). It is referred to ${}^4\text{T}_{1g}(\text{F}) \rightarrow {}^4\text{T}_{2g}(\text{F})$ (ν_1), ${}^4\text{T}_{1g}(\text{F}) \rightarrow {}^4\text{A}_{2g}(\text{F})$ (ν_2) and ${}^4\text{T}_{1g}(\text{F}) \rightarrow {}^4\text{T}_{1g}(\text{p})$ (ν_3) transition respectively, which are typical of stereo geometry of the octahedral. Based on these and elemental (C.H.N) analytical results, FT-IR spectrum, and flame atomic absorption measurements, the structure around the ion of the Co(II) can be suggested as octahedral. The electronic spectrum of $[\text{Cu}(\text{L})_2(\text{Cl})_2]$ complex (Fig. 7) showed a broad absorption band at 700 nm (14285 cm^{-1}), which referred to ${}^2\text{E}_g \rightarrow {}^2\text{T}_{2g}$ transition, This band position is in good accord with the configuration of the octahedral. Therefore we can suggest an octahedral structure around the Cu(II) ion from the above data and those obtained from elementary analysis(C.H.N.), FT-IR, and flame atomic absorption. The electronic spectrum of $[\text{Ni}(\text{L})_2(\text{Cl})_2]$ complex (Fig. 8), shows two bands, at 662 nm (15105 cm^{-1}) and 392 nm (25510 cm^{-1}) assigned to ${}^3\text{A}_{2g} \rightarrow {}^3\text{T}_{1g}(\text{F})$ (ν_2) and ${}^3\text{A}_{2g} \rightarrow {}^3\text{T}_{1g}(\text{P})$ (ν_3) transitions respectively. Those bands show a geometry around an octahedral structure. Octahedral geometry around the ion of Ni(II) may be recommended in the results and those from elementary analysis (C.H.N.), FT-IR spectrum, and flame atomic absorption studies.

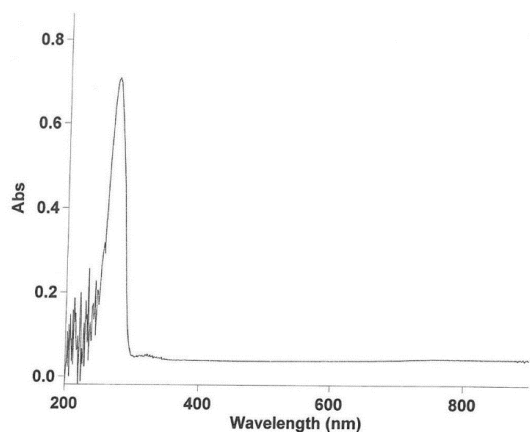


Fig. 5 The UV- Vis spectra of ligand

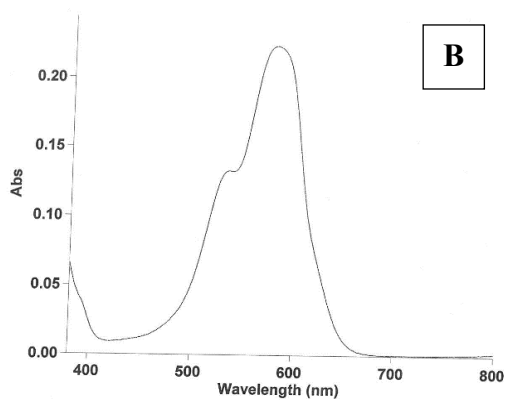
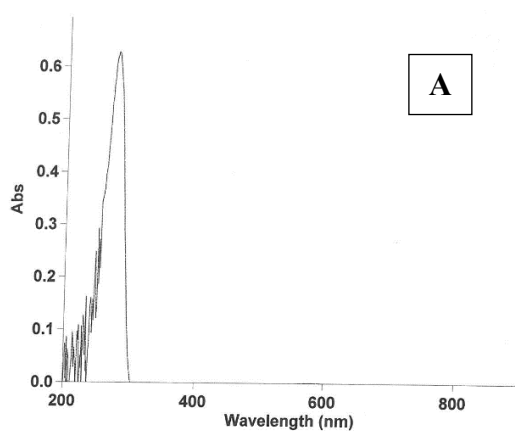


Fig. 6. A) The UV-Vis spectra of $[\text{Co}(\text{L})_2(\text{Cl})_2]$ complex at low concentration and B) only Visible spectra at high concentration

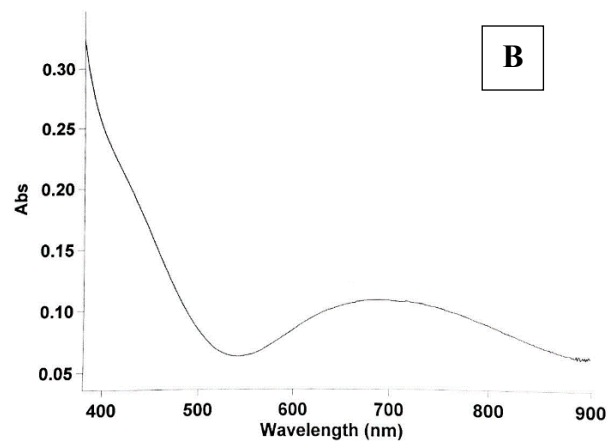
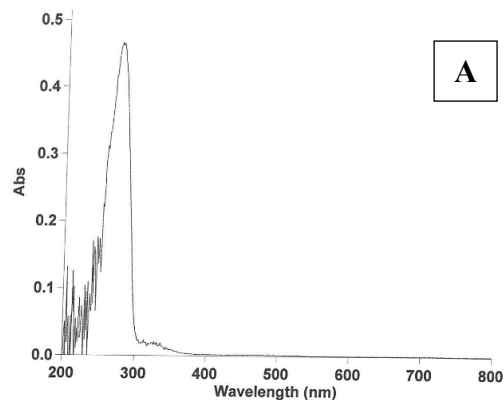
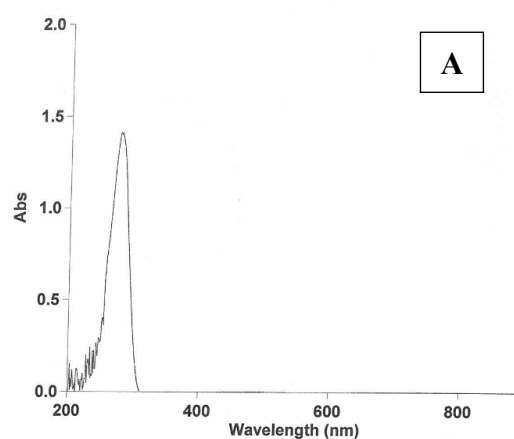


Fig. 7. A) The UV-Vis spectra of $[\text{Cu}(\text{L})_2(\text{Cl})_2]$ complex at Low concentration and B) only Visible spectra at high concentration



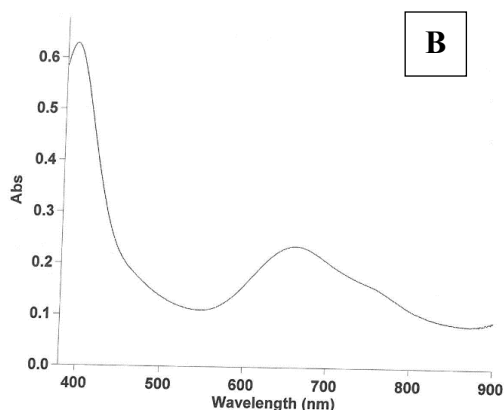


Fig. 8. A) The UV-Vis spectra of $[\text{Ni}(\text{L})_2(\text{Cl})_2]$ complex at low concentration and B) only Visible spectra at high concentration

3.1.2 ^1H NMR spectra of the ligand

The NMR ligand spectrum was measured using the Bruker Advance 400 NMR spectrometer in dimethyl sulfoxide solution (DMSO-d_6). In (Fig. 9) the ligand chemical shifts (δ) are described. We noted that the signal observed at **9.33 ppm** corresponds to the proton of the $\text{CH}=\text{N}$ group. The aromatic proton was observed as multiple at **(7.46–8.51) ppm**, which indicates the hydrogen of an aromatic ring. We also noted the appearance of a singlet at **3.87 ppm** and **4.48 ppm** matching the two groups of methyl ($\text{N}_1\text{-CH}_3$ and $\text{N}_3\text{-CH}_3$) imidazole proton.

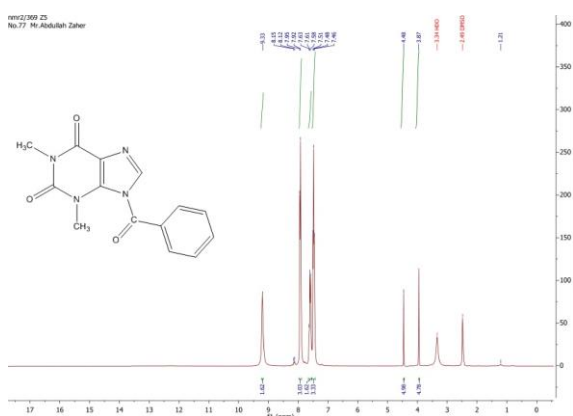


Fig. 9 ^1H NMR spectrum of the new Ligand in DMSO-d_6

3.2 Physical properties and elemental analysis of the ligand and its metal nano complexes

The physical properties, elemental analysis, and metal content of complexes are described in (Tables 1, 2, and 3). The elemental analysis (C.H.N) was performed to the ligand and its metal nano complexes to determine their structural molecular formula through a convergence of theoretical values with the practical values. The metal ion percentage of the complexes was determined using the atomic absorption methods. Most of these results were in good agreement with the theoretical values. Analytical data suggest that the L: M ratio is (2:1) for all complexes. The octahedral structure was suggested according to the previous measurements.

Table 1 Elements analysis and atomic absorption spectroscopy for ligand and its metal nano complexes

Prepared Nano complex	Molecular formula	M.wt g.mol	Metal analyses % Found (calc.)			
			C	H	N	M
L	$\text{C}_{14}\text{H}_{12}\text{N}_4\text{O}_3$	284	59.155 (59.12)	4.225 (4.35)	19.718 (18.55)	-----
$[\text{Co}(\text{L})_2(\text{Cl})_2]$	$\text{C}_{14}\text{H}_{12}\text{N}_4\text{O}_3\text{CoCl}_2$	697.8	48.15 (48.20)	3.44 (3.32)	16.05 (16.01)	8.45 (8.22)
$[\text{Cu}(\text{L})_2(\text{Cl})_2]$	$\text{C}_{14}\text{H}_{12}\text{N}_4\text{O}_3\text{CuCl}_2$	702.4	47.83 (47.52)	3.417 (3.13)	15.94 (14.79)	9.05 (9.02)
$[\text{Ni}(\text{L})_2(\text{Cl})_2]$	$\text{C}_{14}\text{H}_{12}\text{N}_4\text{O}_3\text{NiCl}_2$	697.6	48.16 (48.23)	3.44 (3.32)	16.06 (16.02)	8.42 (8.13)

Furthermore, the molar conductance values of ligand and its metal nanocomplexes were measured in DMSO as a solvent at a concentration of (10^{-3}M), the results appear low values of molar conductivity ($8.65\text{--}13.36 \Omega^{-1}\cdot\text{cm}^2\cdot\text{mole}^{-1}$) which show that all chlorine ions Involved to coordination Table (2). The solubility of ligand and its metal nano complexes at room temperature was examined using different solvents as illustrative in Table (3).

Table 2 Molar conductance of the prepared metal nano complexes

Prepared Nano complexes	Color	Molar Cond. $\Omega^{-1} \cdot \text{cm}^2 \cdot \text{mole}^{-1}$
[Co (R) ₂ (Cl) ₂]	Pink	8.65
[Cu (R) ₂ (Cl) ₂]	Greenish blue	13.36
[Ni (R) ₂ (Cl) ₂]	light blue	10.62

3.3. TEM Measurement

The metal nanocomplexes prepared were measured by the transmission electron microscope. The results show a clear picture of the prepared nanoparticles with a different approximation scale, as shown in (Figs.10-12). All the prepared nanoparticles show empty from any conglomerate, and the dimensions in all synthesised complexes are within the nanoscale (less than 100 nm) which indicates that the kind of nano is particles and zero dimension which is more preferred in preparing nanoscales. The average size was calculated randomly from the figures, as shown in Table (4).

Table 4 Average size nano complexes investigated by TEM

Complexes formula (Nano scales)	ave. Particles size (nm)
[Ni (L) ₂ (Cl) ₂]	18
[Co (L) ₂ (Cl) ₂]	15
[Cu (L) ₂ (Cl) ₂]	12

3.4 Antibacterial activity

Antibacterial activity of the ligand and their metal nanocomplexes were examined against certain bacteria, for example, *Staphylococcus aureus*, *Bacillus subtilis* (Gram-positive bacteria) and *Klebsiella pneumonia*, *Escherichia Coli* (Gram-negative bacteria). The bactericidal examination data of the metal nanocomplexes are in (Table 5) and shown in (Fig. 13). Significant bactericidal properties in the synthesised nano complexes. Comparisons of the biological activities of prepared metal nano complexes with ligand have demonstrated a high significance of complexes compared to other compounds against *Staphylococcus aureus*, *Bacillus subtilis*, *Klebsiella pneumonia*, and *Escherichia Coli*.

Table 3 The solubility of ligand and metal nano complexes

Nano complexes	DMSO	Cold water	Hot water (above 40°C)	Acetone	EtOH	CHCl ₃	MeOH
[Co (L) ₂ (Cl) ₂]	++	-	+	-	-	-	+
[Cu (L) ₂ (Cl) ₂]	++	+	-	-	-	-	-
[Ni (L) ₂ (Cl) ₂]	++	+	++	-	-	-	-
Ligand	++	+	++	+	++	+	++

Where: (++) High solubility, (+ Partial solubility), (- insoluble).

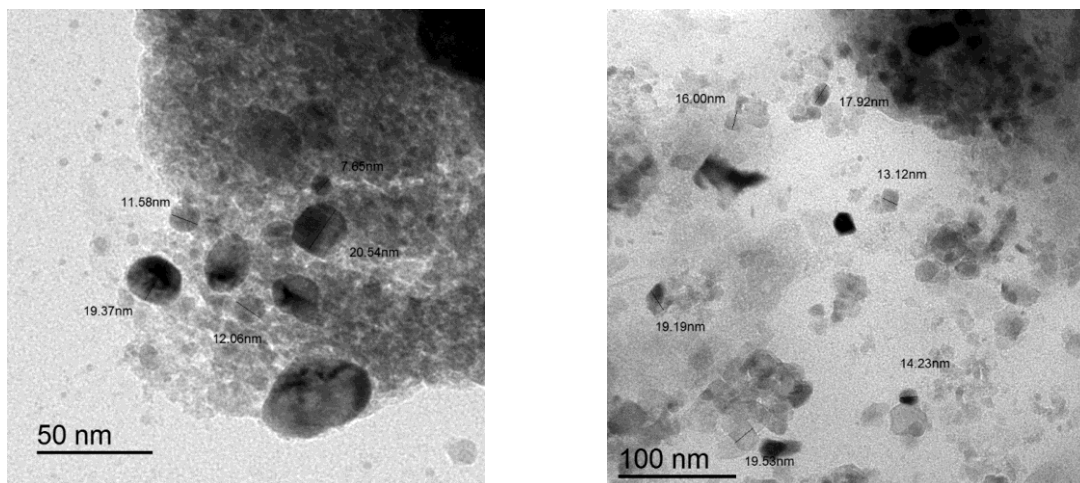


Fig. 10 TEM of $[\text{Co}(\text{L})_2(\text{Cl})_2]$ metal nanocomplex.

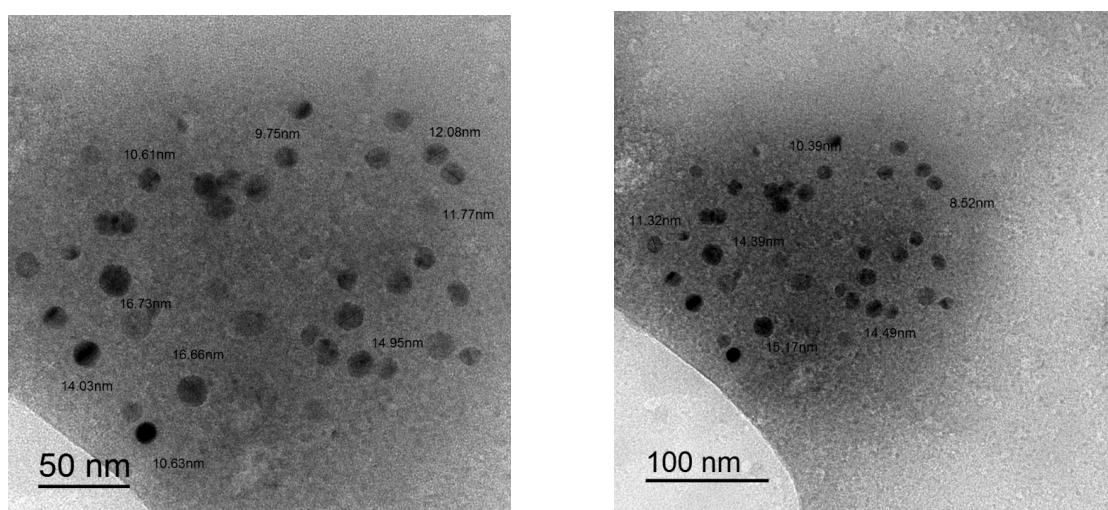


Fig. 11 TEM of $[\text{Cu}(\text{L})_2(\text{Cl})_2]$ metal nanocomplex.

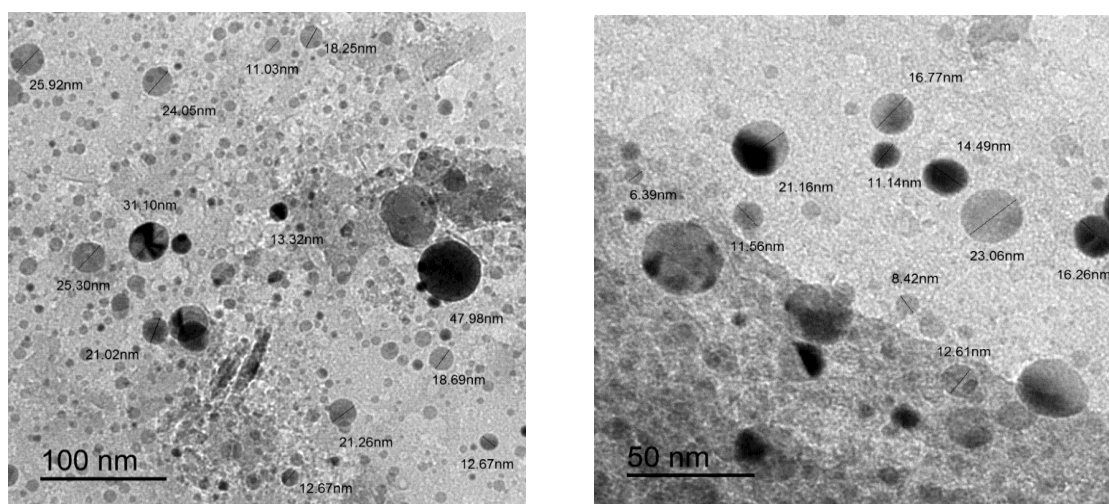


Fig. 12 TEM of $[\text{Ni}(\text{L})_2(\text{Cl})_2]$ metal nanocomplex.

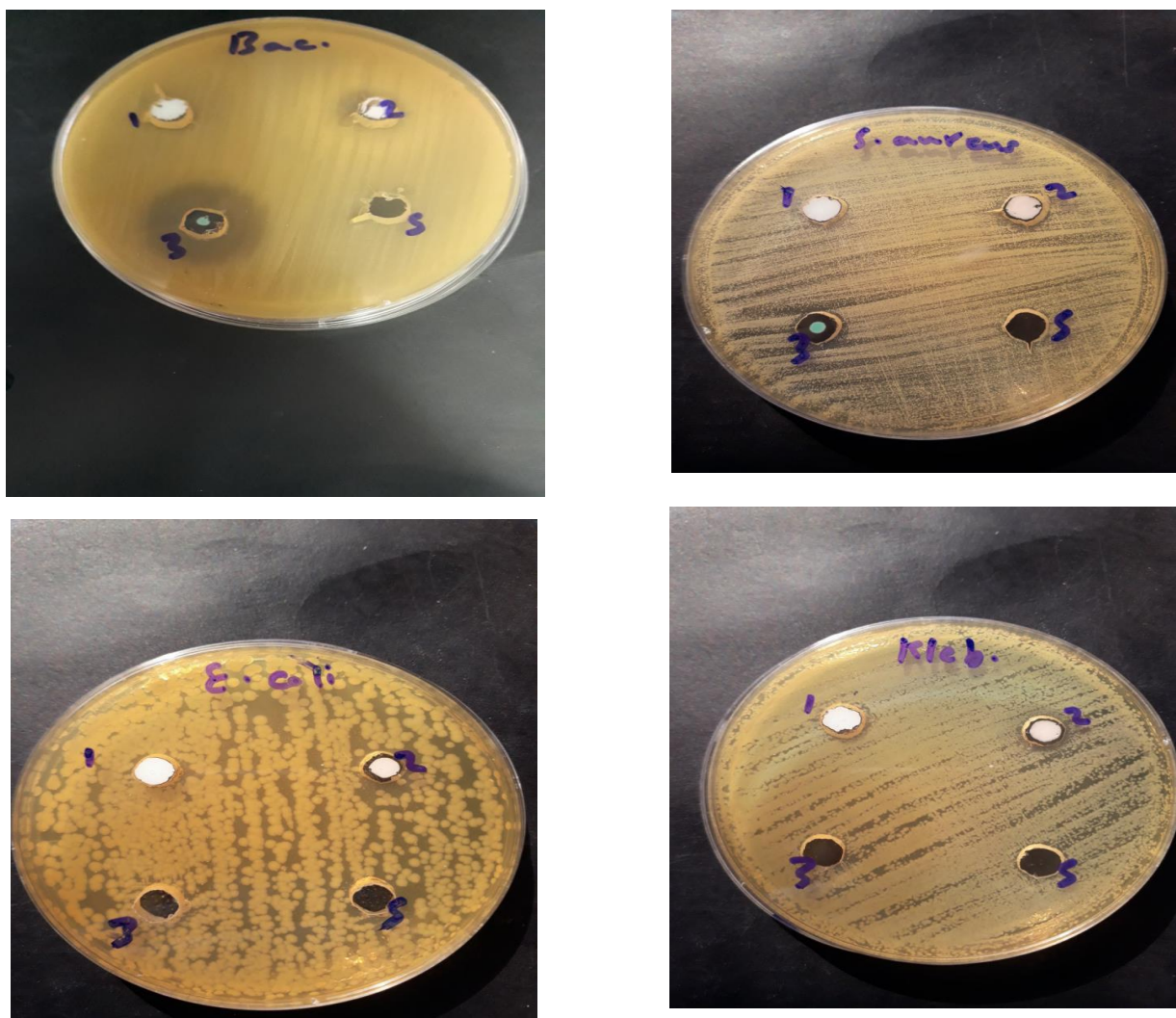


Fig. 13 The activity of metal nano complexes against bacteria

Table 5 The effect of metal nano complexes is represented by inhibition zone (mm) against different bacterial species

Complexes formula (Nano scales)	Staphylococcus aureus	Escherichia Coli	Bacillus subtilis	Klebsiella pneumoniae
[Ni (L) ₂ (Cl) ₂] (1)	7	2	2	3
[Co (L) ₂ (Cl) ₂] (2)	9	5	4	4
[Cu (L) ₂ (Cl) ₂] (3)	12	4	7	2
Ligand(S)	-	-	-	-
DMSO	-	-	-	-

4. Conclusions

A series of new ligand and nano complexes of Co(II), Cu(II) and Ni(II) were synthesised and characterised by both chemical and spectroscopic analysis; Our method (ultrasonic sonication method) Which was used in the synthesis of nanocomplexes has an exhibit that the nanocomplexes can easily be synthesised without aggregation. The complexes were characterised by molar conductance, solubility, atomic flame absorption, (C.H.N) elemental analysis, FT-IR, UV – Vis Spectroscopy that proved an octahedral geometry around the Co (II), Cu (II) and Ni (II). Metal ions are bound to the imidazole ring's nitrogen N7 and O6 atoms. The conductivity data shows that all complexes are non-electrolytic. According to the TEM calculation, the rate size of nano complexes was to be range (12-18) nm. Additionally, Co(II), Cu(II) and Ni(II) complexes exhibited antibacterial activity against Gram-positive bacteria and Gram-negative bacteria higher than ligand.

Acknowledgements

This work was supported by Mustansiriyah University - college of science - Department of Chemistry.

References

- Gacki M, Kafarska K, Pietrzak A, Korona-Głowniak I, Wolf WM. Synthesis, characterisation, crystal structure and biological activity of metal (II) complexes with Theophylline. *Journal of Saudi Chemical Society*. 2019 Mar 1;23(3):346-54.
- Shyاملal BR, Mathur M, Yadav DK, Chaudhary S. Microwave-assisted modified synthesis of C8-analogues of naturally occurring methylxanthines: Synthesis, biological evaluation and their practical applications. *Fitoterapia*. 2020 Mar 4:104533
- Hajji L, Saraiba-Bello C, Segovia-Torrente G, Scalambra F, Romerosa A. CpRu Complexes Containing Water Soluble Phosphane PTA and Natural Purines Adenine, Guanine and Theophylline: Synthesis, Characterisation, and Antiproliferative Properties. *European Journal of Inorganic Chemistry*. 2019 Oct 17;2019(38):4078-86.
- Gacki M, Kafarska K, Pietrzak A, Korona-Głowniak I, Wolf WM. Double Palindrome Water Chain in Cu (II) Theophylline Complex. Synthesis, Characterisation, Biological Activity of Cu (II), Zn (II) Complexes with Theophylline. *Crystals*. 2020 Feb;10(2):97
- Ismail AH, Al-Bairmani HK, Abbas ZS, Rheima AM. Nanoscale Synthesis of Metal (II) Theophylline Complexes and Assessment of Their Biological Activity. *Nano Biomed. Eng*. 2020;12(2):139-47
- Ismail AH, Al-Bairmani HK, Abbas ZS, Rheima AM. Synthesis, Characterization, Spectroscopic and Biological Studies of Zn (II), Mn (II) and Fe (II) Theophylline Complexes in Nanoscale. *Nano Biomed. Eng*. 2020 Jul 1;12(3):253-61.
- Ismail AH, Al-Bairmani HK, Abbas ZS, Rheima AM. Synthesis, characterisation, spectroscopic, and biological activity studies of Nano scale Zn(II), Mn (II) and Fe (II) theophylline complexes. *Journal of Xi'an University of Architecture & Technology*. 2020; XII (II): 2775-2789.
- Ismail AH, Al-Bairmani HK, Abbas ZS, Rheima AM. Nano metal-complexes of

- theophylline derivative: synthesis, characterization, molecular structure studies, and antibacterial activity. In IOP Conference Series: Materials Science and Engineering 2020 Nov 1 (Vol. 928, No. 5, p. 052028). IOP Publishing.
- Kistenmacher, Thomas J., et al. "The N (7), O (6) chelation mode of 6-oxopurines. Preparation and structure of (N-salicylidene-N', N'-dimethylethylenediamine)(theophyllinato) copper (II)-3.5-water." *Inorganic Chemistry* 17.9 (1978): 2582-2584.
 - Cozak, Daniel, et al. "N7/O6 chelation in a complex with an analog of guanine. Preparation, spectroscopic study, and crystal structure of bis (. eta. 5-cyclopentadienyl)(theophyllinato) titanium (III)." *Inorganic Chemistry* 25.15 (1986): 2600-2606.
 - Abdulah HI, Hussain DH, Rheima AM. Synthesis of α -Fe₂O₃, γ -Fe₂O₃ and Fe₃O₄ Nanoparticles by Electrochemical Method. *Journal of Chemical, Biological and Physical Sciences*. 2016; 6(4):1288-1296
 - Mohammed MA, Rheima AM, Jaber SH, Hameed SA. The removal of zinc ions from their aqueous solutions by Cr₂O₃ nanoparticles synthesised via the UV-irradiation method. *Egyptian Journal of Chemistry*. 2020 Feb 1;63(2):5-6.
 - Rheima AM, Mohammed MA, Jaber SH, Hasan MH. Inhibition effect of silver-calcium nanocomposite on alanine transaminase enzyme activity in human serum of Iraqi patients with chronic liver disease. *Drug Invention Today*. 2019 Nov 15;12(11).
 - Rheima, A.M., D.H. Hussain, and H.I. Abdulah, *Silver nanoparticles: Synthesis, Characterisation and their used a counter electrodes in novel Dye sensitiser solar cell*. IOSR Journal of Applied Chemistry, 2016. 9(10): p. 6-9.
 - Hussain DH, Rheima AM, Jaber SH, Kadhim MM. Cadmium ions pollution treatments in aqueous solution using electrochemically synthesised gamma aluminum oxide nanoparticles with DFT study. *Egyptian Journal of Chemistry*. 2020 Feb 1;63(2):417-24
 - Rheima AM, Hussain DH, Almjibilee MM. Graphene-Silver Nanocomposite: Synthesis, and Adsorption Study of Cibacron Blue Dye from Their Aqueous Solution. *Journal of Southwest Jiaotong University*. 2019;54(6).
 - Hussain DH, Abdulah HI, Rheima AM. Synthesis and Characterisation of γ -Fe₂O₃ Nanoparticles Photo Anode by Novel Method for Dye Sensitized Solar Cell. *International Journal of Scientific and Research Publications*. 2016;6(10):26-31.
 - Kadhun HA, Salih WM, Rheima AM. Improved PSi/c-Si and Ga/PSi/c-Si nanostructures dependent solar cell efficiency. *Applied Physics A*. 2020 Oct;126(10):1-5.
 - Rheima AM, Hussain DH, Abed HJ. Fabrication of a new photo-sensitized solar cell using TiO₂/ZnO Nanocomposite synthesized via a modified sol-gel Technique. In IOP Conference Series: Materials Science and Engineering 2020 Nov 1 (Vol. 928, No. 5, p. 052036). IOP Publishing.
 - Aboud NA, Alkayat WM, Hussain DH, Rheima AM. A comparative study of ZnO, CuO and a binary mixture of ZnO. 5-CuO. 5 with nano-dye on the efficiency of the dye-sensitized solar cell. In *Journal of Physics:*

- Conference Series 2020 Nov 1 (Vol. 1664, No. 1, p. 012094). IOP Publishing.
21. Rheima AM, Mohammed MA, Jaber SH, Hameed SA. Adsorption of selenium (Se⁴⁺) ions pollution by pure rutile titanium dioxide nanosheets electrochemically synthesized. *Desalination and Water Treatment*. 2020 Aug 1;194:187-93.
 22. Jasim NA, Al-Gasha'a FA, Al-Marjani MF, Al-Rahal AH, Abid HA, Al-Kadhmi NA, Jakaria M, Rheima AM. ZnO nanoparticles inhibit growth and biofilm formation of vancomycin-resistant *S. aureus* (VRSA). *Biocatalysis and Agricultural Biotechnology*. 2020 Oct 1;29:101745.
 23. Rheima AM, Mahmood R S, Hussain DH, Abbas ZS. Study the Adsorption Ability of Alizarin Red Dye From Their Aqueous Solution on Synthesized Carbon Nanotubes. *Digest Journal of Nanomaterials and Biostructures*. 2020;15(4).
 24. Ali AA, Al-Hassani RM, Hussain DH, Rheima AM, Abd AN, Meteab HS. Fabrication of Solar Cells Using Novel Micro-and Nano-Complexes of Triazole Schiff Base Derivatives. *Journal of Southwest Jiaotong University*. 2019;54(6).
 25. Ali AA, Al-Hassani RM, Hussain DH, Rheima AM, Meteab HS. Synthesis, spectroscopic, characterisation, pharmacological evaluation, and cytotoxicity assays of novel nano and micro scale of copper (II) complexes against human breast cancer cells. *Drug Invention Today*. 2020; 14(1).
 26. Warra, A. A. "Transition metal complexes and their application in drugs and cosmetics-a Review." *Journal of Chemical and Pharmaceutical Research* 3.4 (2011): 951-958.
 27. Qiu K, Zhu H, Rees TW, Ji L, Zhang Q, Chao H. Recent advances in lysosome-targeting luminescent transition metal complexes. *Coordination Chemistry Reviews*. 2019 Nov 1;398:113010.
 28. Rafique, Shazia, et al. "Transition metal complexes as potential therapeutic agents." *Biotechnology and Molecular Biology Reviews* 5.2 (2010): 38-45.
 29. Rheima AM, Mohammed MA, Jaber SH, Hameed SA. Synthesis of silver nanoparticles using the UV-irradiation technique in an antibacterial application. *Journal of Southwest Jiaotong University*. 2019;54(5).
 30. Rheima AM, Aboud NA, Jasim BE, Ismail AH, Abbas ZS. Synthesis and structural characterization of ZnTiO₃ nanoparticles via modification sol-gel processes for assessment of their antimicrobial activity. *International Journal of Pharmaceutical Research*. 2021; 13(1).
 31. Jabber SH, Hussain DH, Rheima AM, Faraj M. Comparing study of CuO synthesized by biological and electrochemical methods for biological activity. *Al-Mustansiriyah Journal of Science*. 2019;30(1):94-8.